Structure of *Pseudomonas aeruginosa* Zinc-Azurin Mutant Asn47Asp at 2.4 Å Resolution

By Lennart Sjölin,* Li-Chu Tsai and Vratislav Langer

Department of Inorganic Chemistry, Chalmers University of Technology and the University of Göteborg, S-412 96 Göteborg, Sweden

Torbjörn Pascher, Göran Karlsson and Margareta Nordling

Department of Biochemistry and Biophysics, University of Göteborg, S-412 96 Göteborg, Sweden

and Herbert Nar

Max Planck Institut für Biochemie, Abteilung für Strukturforschung, Martinsried bei München, Germany

Abstract

The *Pseudomonas aeruginosa* azurin mutant Asn47Asp has been isolated, its spectroscopic and kinetic properties characterized, and the X-ray crystal structure of its zinc derivative determined. While the optical and electron paramagnetic resonance spectra as well as the electron-transfer activity of the mutant are very similar to the wild-type values, the Asn47Asp reduction potential is slightly increased by 20 mV. The mutant crystallized in the orthorhombic space group $P2_12_12_1$ with cell dimensions $a = 57.8$, $b = 81.5$ and $c = 112.6$ Å. There are four molecules in the asymmetric unit, packed as a tetramer which consists of two independent dimers. The zinc site of this mutant structure is similar to the wild-type zinc azurin and, in particular, the metal-binding site is almost identical to the site found in the wild-type zinc-azurin structure [Nar, Huber, Messerschmidt, Filippou, Barth, Jaquinod, Kamp & Canters (1992). *Eur. J. Biochem.* **205**, 1123–1129]. The Asp47 side chain at that mutation site takes on a very similar orientation to Asn47 in the wild-type structure preserving the two hydrogen bonds with the neighbouring Thr113 NH and O^γH. Therefore, the increased reduction potential of the mutant is probably a result of an altered charge distribution close to the metal site.

Introduction

Azurin is a bacterial electron-transfer protein containing a single blue or type I Cu^{II} ion (Malkin & Malmström, 1970; Fee, 1975). The group of blue copper proteins to which azurin belongs has attracted a lot of attention recently because of some rather unusual spectroscopic properties and because of their model character in biological electron transfer (Adman, 1991; Solomon & Lowery, 1993). The type I copper proteins show an intense absorption band near 600 nm, a narrow hyperfine splitting in the EPR (electron paramagnetic resonance) signal and a high reduction potential of 200–400 mV. Various other spectroscopic methods, such as EPR, CD (circular dichroism), EXAFS (extended X-ray absorption fine-structure spectroscopy), resonance Raman spectroscopy and NMR have been used to study these proteins (Ainscough *et al.*, 1987; Blair *et al.*, 1985; Groeneveld & Canters, 1985).

In the different families of blue copper proteins there is a high degree of homology and many amino-acid residues are conserved, particularly near the copper-binding site (Rydén, 1984). The copper ligands, two histidine residues and one cysteine residue (NNS) were unambiguously determined from the crystal structure of *Populus nigra italica* plastocyanin (Guss & Freeman, 1983). This copper-site geometry was confirmed from the crystal structure of azurin from *Pseudomonas aeruginosa* (Adman & Jensen, 1981) and *Alcaligenes denitrificans* (Norris, Anderson & Baker, 1986; Baker, 1988). The three ligands are conserved in all blue copper proteins. A fourth ligand, a methionine, has also been indicated but it is not at all certain to what extent this methionine is to be regarded as a true ligand. Even if this amino-acid residue is conserved in most of the blue copper proteins, it is missing in at least two proteins: *Rhus vernicifera* stellacyanin and *Neurospora crassa* laccase. In most of the type I copper structures now known, the methionyl S-atom distance is very long, in the range of 2.9–3.4 Å, the only exception being the distance of 2.76 Å in pseudoazurin (Petratos, Dauter & Wilson, 1988). In addition, there is an

---

* Author for correspondence.

indication of a plausible fifth ligand, a carbonyl O atom from Gly45, but once again this ligand is also at a very long distance. Consequently, the azurin copper site can be approximated to an irregular trigonal bipyramid with two weakly interacting groups in the axial positions (Nar, Messerschmidt, Huber, van de Kamp & Canters, 1991a,b).

The idea of the rack mechanism for proteins and enzymes was introduced by Lumry & Eyring (1954). According to this hypothesis, key functional groups can be held in distorted positions by the overall protein conformation, this in turn leading to anomalous properties. This concept was further discussed and developed by Eyring, Lumry & Spikes (1956) and other experimental support for this concept was soon obtained, particularly from investigations of metalloenzymes (Lindskog & Malmström, 1962). It was also found that a number of copper proteins, active in electron-transfer reactions, could be characterized by their unique spectroscopic parameters (Malmström & Vänngård, 1960; Malmström, 1965). A similar concept, the entatic nature of the metal site, was later discussed by Vallee & Williams (1968). Entatic, from the greek word 'entasis', literally means a stretched state or a state under tension. Gray & Malmström (1983) used the spectroscopic data available at that time to estimate the rack- or entatic state energy of a blue copper site, and in this case the plastocyanin protein in particular was investigated. They concluded their analysis with a statement that the distorted site geometry of blue copper centres (enforced by the protein) is not only responsible for the high reduction potentials and facile electron-transfer kinetics, but apparently also provides an attractive way to tune potentials further.

In order to investigate the fundamentals of the rack mechanism in more detail we have published the results from cassette-mutagenesis experiments on the methionine ligand in azurin from *Pseudomonas aeruginosa* (Karlsson, Nordling, Pascher, Tsai, Sjölin & Lundberg, 1991). The spectroscopic properties of these mutant proteins vary considerably, and the reduction potentials span a range of 250 mV (Pascher, Karlsson, Nordling, Malmström & Vänngård, 1993). The crystal structure of the mutant Met121Glu has, in addition, been determined (Karlsson, Tsai, Nar, Langer & Sjölin, 1993) and the spectroscopic properties and the reduction potentials discussed in view of the structure of the copper site. In particular, it was found in the latter investigation that the exchange of the conserved methionine of the type I copper site only induces a large change in the geometry of the mutated side chain, and consequently large changes in the spectroscopic properties and reduction potential of the copper site, confirming the concept of the rack mechanism in the small blue copper proteins.

Recently, *Pseudomonas aeruginosa* zinc azurin has been isolated as a by product of heterologous expression of copper azurin in *Escherichia coli* (Nar et al., 1992). It was inferred that, despite the high selectivity of apo-azurin for Cu^{II} over Zn^{II}, Zn^{II} contamination in recombinant azurin preparations could be as high as 50%. The structure analysis of zinc azurin showed that zinc binds in a distinctly different mode to azurin, mainly because of the location of Zn^{II} at only 2.3 Å from the carbonyl O atom of Gly45, which is around 3 Å from Cu^{II} in copper azurin. The coordination sphere of Zn^{II} in azurin is distorted tetrahedral and based on the strongly bound His46, His117 and Cys112 ligands in addition to the O atom of Gly45.

The zinc-azurin mutant Asn47Asp represents a group of mutants where the mutation site is thought to affect the metal site indirectly *via* an elaborate hydrogen-bond pattern and consequently the reduction potential will also be changed if the Asn47 side chain is mutated. Asn47 was also of interest as a mutation site since this amino-acid residue is invariant and conserved in all blue copper proteins sequenced so far (Chothia & Lesk, 1982; Rydén & Lundgren, 1976; Ambler & Tobari, 1985; van Beeumen, van Bun, Canters, Lommen & Chothia, 1991). The Asn47 side chain forms two strong hydrogen bonds with the neighbouring residue Thr113 NH and $O^{\gamma}H$, thereby connecting two ligand-bearing β-strands of the eight-stranded azurin β-barrel. These hydrogen bonds are probably important for the rigidity of the metal site and thereby any change would ultimately lead to a difference in the entatic state or rack energy. In this respect, the replacement of copper in the metal site with zinc also contributes to the understanding of the nature of the rack mechanism.

A report has recently been published on the *Alcaligenes denitrificans* azurin mutant Asn47Leu in which both hydrogen bonds have been abolished (Hoitink & Canters, 1992). The mutant retains most of the characteristic spectroscopic features of wild-type azurin, but has a lower thermal stability and a sharply increased midpoint potential ($\Delta E = 110$ mV). In Asp47 azurin, the two hydrogen-bond acceptors are still available leaving the possibility of an isosteric structure. However, we decided to study the effect of a negative charge introduced into the protein interior close to the metal-binding site by the Asn47Asp mutation.

Here we describe the crystallization, crystallographic analysis and the refinement of the *Pseudomonas aeruginosa* zinc-azurin mutant Asn47Asp at 2.4 Å resolution. The structure is compared with the wild-type azurin structure and the differences are viewed against the differences in some of the biophysical properties for the Asn47Asp mutant.

Materials and methods

Site-directed mutagenesis and preparation of azurins

Escherichia coli K12 strain TG1 (Carter, 1986) was used both for cloning and protein production. The plasmids pUC18/19 and M13mp18/19 were purchased from Boehringer–Mannheim. The plasmid pUG4 has been described earlier (Karlsson, Pascher, Nordling, Arvidsson & Lundberg, 1989) as have the DNA technique, the production and the purification of the recombinant *Pseudomonas aeruginosa* azurin and mutants (Pascher, Bergström, Malmström, Vänngård & Lundberg, 1989).

Optical and EPR spectra and reduction potential

Optical spectra were recorded with a Shimadzu 3000 spectrophotometer. EPR spectra were obtained on a Bruker ER 20D-SRC spectrometer equipped with an Oxford Instruments EPR-9 helium cryostat. The optical spectra were recorded at a temperature of 20 K. Integrations were performed as described by Aasa & Vänngård (1975).

The reduction potentials were determined by Karlsson, Pascher, Nordling, Arvidsson & Lundberg (1989), but at 298 K and with the redox mediator tris(1,10-phenanthroline)cobalt(III) perchlorate. Both azurin and the mediator had a concentration of 1 mM (Sailasuta, Anson & Gray, 1979). A detailed presentation has been published by Pascher (1992).

Crystallization and data collection

Prism-like Asn47Asp crystals were formed from a solution containing 3.6 M ammonium sulfate, 0.5 M lithium nitrate and 0.1 M acetate buffer at pH 5.7 and at the temperature of 297–298 K in about 10 d. The largest crystal of this form was about 0.4 × 0.2 × 0.1 mm. This crystallization procedure is similar to the one used by Adman, Stenkamp, Sieker & Jensen (1978).

The diffraction data were collected using a Siemens electronic area detector. X-rays (Cu $K\alpha$ radiation) were generated with a Rigaku RU200 BH rotating anode operated at 40 kV and 80 mA with a 0.3 × 0.3 mm focal spot. A graphite monochromator together with a 0.5 mm collimator were also used. During the data collection the area-detector chamber was mounted 9 cm from the crystal and the data set was collected at room temperature. The individual frames were contiguous in that the beginning of each small oscillation range (0.1°) coincided with the end of the previous range. The determination of the unit-cell parameters, crystal orientation and the integration of reflection intensities were performed with the *XENGEN* program system (Howard, Gilliland, Finzel, Poulos, Ohlendorf & Salemme, 1987). The mutant Asn47Asp crystals belong to the ortho-

rhombic system and the space group has been determined as $P2_12_12_1$. The cell parameters are $a = 57.8$, $b = 81.5$ and $c = 112.6$ Å, $V = 531\,000$ Å³. The final data set after internal scaling consisted of 17 198 reflections to 2.4 Å resolution. The data set represents 83% of the expected number of reflections at this resolution. In the entire data set 14 916 reflections had intensities greater than σ_I, 13 633 reflections had intensities greater than $2\sigma_I$ and 12 549 reflections had intensities greater than $3\sigma_I$, the standard deviation σ_I, being derived from statistical calculations in the *XENGEN* system. The merging R_m factor, $R_m = \sum_h |I_i - I| / \sum_h I$ (I_i is the intensity of an individual measurement, I the mean value for that reflection and the summations are over all measurements), was 6.6% for all that data to 2.4 Å resolution. The fraction of the number of observed reflections with intensities $I > \sigma_I$, as a function of resolution, is given in Fig. 1. The Wilson (1949) distribution is illustrated in Fig. 2 for the total of 17 198 reflections. The fit to the theoretical straight line is satisfactory for a protein data set with the
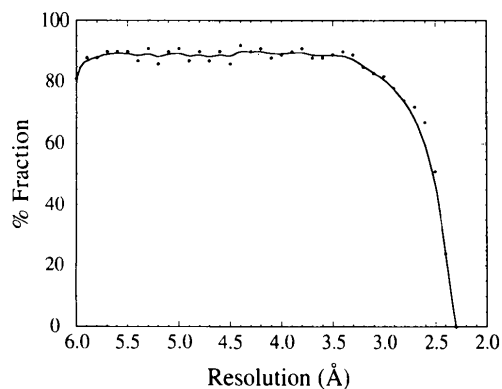

Fig. 1. Fraction of the number of reflections with intensities $I > 3\sigma_I$ as a function of resolution.
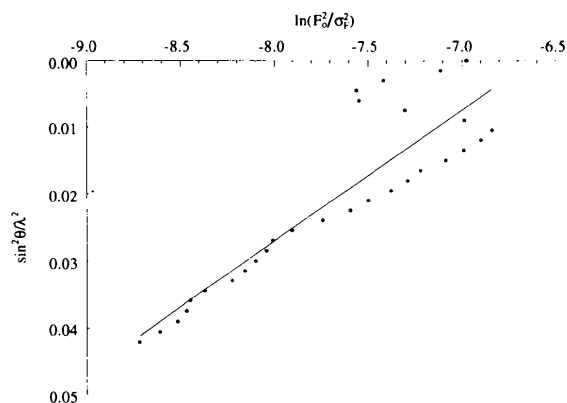

Fig. 2. The Wilson plot for the area-detector data extending to 2.4 Å resolution.

Table 1. *Data-collection parameters and statistics, final model and refinement results for the Asn47Asp zinc derivative mutant*

Unit-cell constants (Å)	a	57.8
	b	81.5
	c	112.6
Space group		$P2_12_12_1$
No. of molecules in asymmetric unit		4
Crystal mosaicity (°)		0.21
Total No. of measurements		80786
Total No. of unique reflections		17198
Data completeness (%)		83
Reflection averaging (%) R_m*		6.6
No. of atoms used in refinement		4169
Protein atoms		3895
Solvent		274
Resolution range used in the refinement (Å)		8.0–2.4
No. of reflections in the resolution range		15541
No. of parameters		16677
Root-mean-square deviation		
bonds (Å)		0.016
angles (°)		2.9
R value ($R = \Sigma|F_o - F_c|/\Sigma|F_o|$) (%)		17.1

* $R_m = \Sigma|I(k) - \langle I\rangle|/\Sigma I(k)$, where $I(k)$ and $\langle I\rangle$ are the intensity values of individual measurements and of the corresponding mean values of independent Friedel pairs and symmetry-related reflections.

expected deviations in the range 4.0–10.0 Å. The overall temperature factor obtained from the slope of the least-squares line, 22.7 Å^2, is somewhat higher than the B value obtained later in the refinement, 17.8 Å^2 on average. The unique reflections were also analyzed using the program *LOAD* from the *PROTEIN* system (Steigemann, 1974), and some of the data-collection statistics are presented in Table 1. There are four molecules in the asymmetric unit and the calculated V_m value is 2.37 Å^3 Da^{-1} (Matthews, 1968).

Structure solution and refinement

The crystal structures of both the oxidized *Pseudomonas aeruginosa* wild-type azurin in addition to the azurin mutants His35Leu and His35Gln have been reported (Nar, Messerschmidt, Huber, van de Kamp & Canters, 1991a,b) and the wild-type crystal form in these investigations was found to be isomorphous with the His35Leu crystal form. Since our crystal form for the oxidized mutant Asn47Asp is also isomorphous with the wild-type azurin solved previously and the His35Leu mutant, the coordinates from the His35Leu mutant, because of their greater accuracy, were selected to be used as the starting set for the subsequent refinement and modelling analysis of the Asn47Asp azurin mutant. Before the crystallographic refinement was initiated the amino-acid residue Leu35 was changed back to histidine and the amino-acid residue Asn47 was consequently changed to aspartic acid. In the first step of the refinement the four molecules in the asymmetric unit, consisting of 3895 non-H atoms in 512 amino acids, were subjec-

ted to a rigid-body least-squares refinement using the *X-PLOR* program (Brünger, 1990). The refinement was performed on 8448 reflections in the resolution range of 6.0–3.0 Å. The crystallographic R value was initially 0.415 but was lowered in 30 successive cycles to 0.241. At this point the resolution range was extended to become 8.0–2.4 Å and the individual atomic positions and temperature factors for the non-H atoms in the model were released. After 80 cycles of Powell refinement of the atomic positions followed by an additional 30 cycles of individual temperature-factor refinement, the R value dropped from 0.301 to 0.213. The model was kept close to standard geometries throughout the refinement by correct weighting.

A regular $2F_o - F_c$ Fourier map was subsequently calculated and the density and the corresponding model were visually inspected. Solvent molecules were now introduced into the model and the water molecules were placed in densities which gave reasonable hydrogen bonds to the protein atoms or to other solvent molecules. In total, 274 water molecules were added after a series of Fourier-map calculations and modelling cycles using the program *FRODO* (Jones, 1978). Side chains that motivated minor modelling were also changed at this stage of the investigation. The final model was then subjected to an additional 80 cycles of Powell positional refinement followed by 30 cycles of individual temperature-factor refinement and the crystallographic R value was lowered to 0.171. The final r.m.s. deviations from ideal bond lengths and angles are 0.016 Å and 2.9°, respectively.
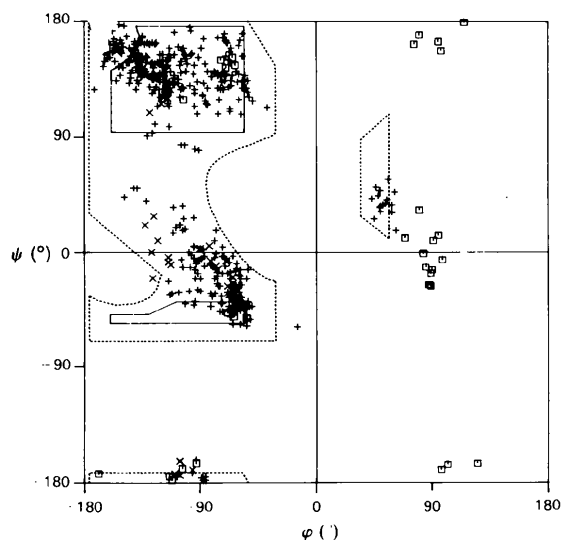

Fig. 3. Ramachandran (φ,ψ) plot of Asn47Asp azurin mutant. Dihedral angle regions for α-helices, β-sheets and left-handed α-helices are indicated. Glycines are represented by rectangles.

The quality of the refined structure is also indicated in the Ramachandran plot, Fig. 3, in which the values of the main-chain torsion angles φ and ψ are plotted pairwise. The sterically allowed regions for all amino acids except glycyl residues are indicated by dashed lines (Ramakrishnan & Ramachandran, 1965). Almost all residues of the protein lie in the allowed regions.

An upper limit for the average coordinate error can be assessed according to Luzzati (1952) by plotting the R factor as a function of resolution (Fig. 4). The data points follow satisfactorily the line drawn for a mean coordinate error of 0.20 Å. However, it is known that the Luzzati plot overestimates the error in the model because it assumes that the disagreement between F_o and F_c is only as a result of the coordinate error.*

Energy-dispersive X-ray fluorescence

The mutant Asn47Asp crystals have been analyzed for trace elements by energy-dispersive X-ray fluorescence, a sensitive non-destructive method (Standzenieks, Rindby & Selin, 1978; Standzenieks & Selin, 1979). In this method, the primary Cu $K\alpha$ radiation from an X-ray tube impinges on a secondary target of molybdenum, the characteristic radiation of which then excites characteristic radiation from the elements in the sample. The X-ray fluorescence spectra of the azurin mutant Asn47Asp is presented in Fig. 5.

---

* Atomic coordinates and structure factors have been deposited with the Protein Data Bank, Brookhaven National Laboratory (Reference: 1AZR, R1AZRSF). Free copies may be obtained through The Technical Editor, International Union of Crystallography, 5 Abbey Square, Chester CH1 2HU, England (Supplementary Publication No. SUP 37087). A list of deposited data is given at the end of this issue.
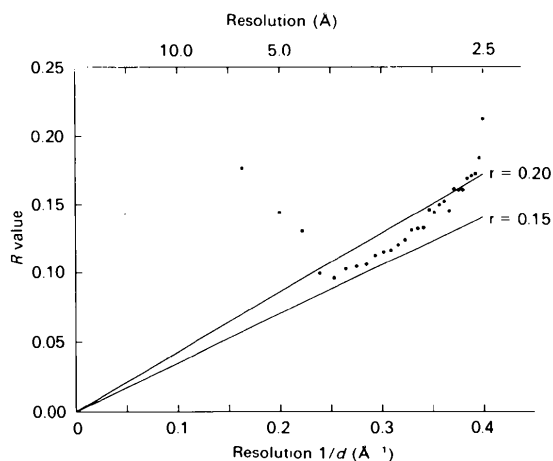
Results

The protein sample of Asn47Asp azurin obtained displayed an unusually weak colouration which could not be increased by the addition of Cu^{II} ions. Considering the results from *Pseudomonas aeruginosa* zinc azurin, we applied energy-dispersive X-ray fluorescence for the analysis of the relative content of Cu^{II} and Zn^{II} in the Asn47Asp sample. The spectrum from the azurin crystal is shown in Fig. 5 and it is clearly seen that the copper content in this particular single crystal of the Asn47Asp zinc mutant is about 3%. However, we considered this impurity of copper to be sufficient to enable further spectroscopic measurements to be performed and also to measure the reduction potential for the copper-containing Asn47Asp mutant. As indicated by Nar *et al.* (1992), zinc azurin, generally called 'azurin*', will not show any reduction potential because of the electronic properties of the Zn atom. Further, the zinc azurin is spectroscopically silent in the visible region of the absorption spectra. From the copper impurity of the crystal, however, the spectroscopic properties for this mutant have been determined and these properties are summarized in Table 2. While spectroscopic and kinetic properties are unchanged with respect to the wild-type azurin, the redox potential in the mutant is slighly increased by 20 mV.

The final model for the Asn47Asp zinc mutant consists of 3895 protein atoms in four crystallographically independent molecules in the asymmetric unit and, in addition, 274 water molecules and the crystallographic R value became 0.171 for 15 541 reflections in the resolution interval 8.0–2.4 Å. The

Fig. 4. Plot of R factor *versus* resolution after Luzzati (1952). All reflections with $F_o > 3\sigma_F$ were used.
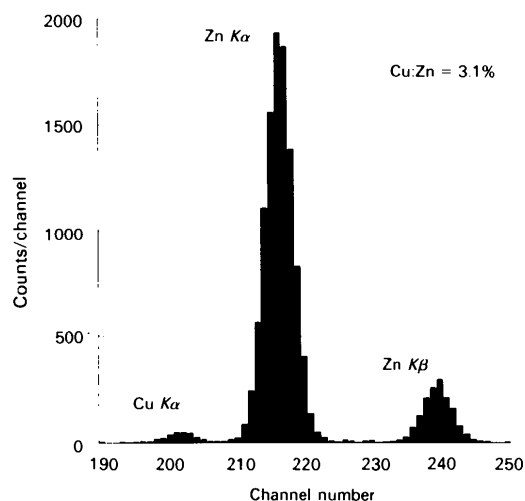

Fig. 5. Results from the analysis of the zinc/copper content in the protein crystal used for the crystallographic data collection using the energy-dispersive X-ray fluorescence technique.

Table 2. *Optical and EPR properties and reduction potentials of wild-type azurin, Asn47Asp mutant and zinc azurin*

$g_{\parallel}$ and $g_{\perp}$ are field vectors and $A_{\parallel}$ is the hyperfine coupling in the parallel direction. ε is the optical absorption coefficient.

(a) Optical and EPR properties

	EPR parameters			λ_{max}	ε
	$g_{\parallel}$	$A_{\parallel}$	$g_{\perp}$	(nm)	$(M^{-1}cm^{-1})$
Wild type	2.259	50	2.059	627.0	5500
Asn47Asp	2.253	53	2.053	623.5	5600
Zinc azurin	—	—	—	628.0*	—

(b) Reduction potentials

	E° (mV) Phosphate pH 7.0
Wild type	310
Asn47Asp	333

* From Nar *et al.* (1992).

Table 3. *R.m.s. deviations calculated from a superposition of each of the four monomers A–D in the Asn47Asp azurin mutant*

The four r.m.s. values per block indicate values for C^{α} atoms, main-chain atoms, side-chain atoms and all atoms.

	A–B	A–C	A–D	B–C	B–D	C–D
C^{α} atoms	0.3562	0.4497	0.3496	0.3409	0.3787	0.3791
Main chain	0.4391	0.5145	0.3605	0.3490	0.4595	0.4887
Side chain	1.1503	1.1511	1.2002	0.9161	1.2297	1.2521
All atoms	0.8535	0.8758	0.8661	0.6795	0.9093	0.9315

Table 4. *Metal-site geometry in the zinc-azurin mutant Asn47Asp compared to wild-type azurin and zinc azurin*

	Zn–ligand bond length (Å)		
	Asn47Asp mutant	Wild-type azurin (pH 5.5)	Zinc derivative azurin
Zn—O(45)	2.36	2.97	2.32
Zn—N$^{\delta 1}$(46)	2.09	2.11	2.07
Zn—S$^{\gamma}$(112)	2.27	2.25	2.30
Zn—N$^{\delta 1}$(117)	2.04	2.03	2.01
Zn—S$^{\delta}$(121)	3.44	3.15	3.38
C$^{\alpha}$(45)—C$^{\alpha}$(121)	11.50	11.65	11.38
O(45)—C$^{\alpha}$(121)	9.19	9.42	9.09

average isotropic temperature factor for the protein atoms was calculated to be 15.7 Å^2 while the average temperature factor for the solvent atoms became 35.8 Å^2 (see Table 1). Further inspection of the temperature factors reveals that most of the Asn47Asp-mutant structure is well defined, especially the β-strands, the loops around the metal site and all internal side chains. The other regions consisting of the N and C terminus and the loops between the β-strands all have higher average temperature factors.

Another measure of the quality of the model is to determine the position of plausible errors in the structure by calculating how well the structure fits the electron-density map on a per-residue basis as suggested by Wirenga, Kalk & Hol (1987) and Jones, Zou, Cowan & Kjeldgaard (1991). The quality of the structure solution as determined by this technique is presented in Fig. 6. A comparison of the four monomers in the asymmetric unit indicates that the deviation of the main-chain atoms in Asn47Asp from the
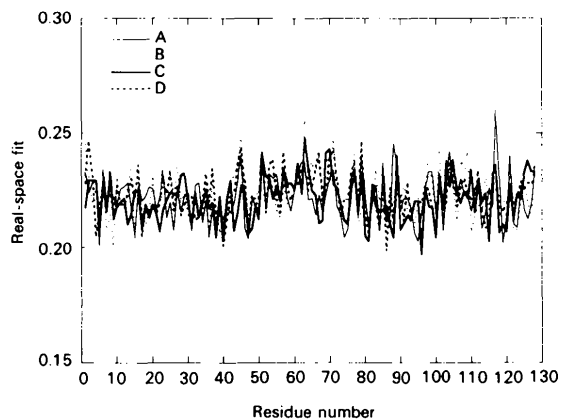

Fig. 6. Plot of main-chain residue real-space-fit residuals for the Asn47Asp azurin mutant. *A*, *B*, *C* and *D* curves represent the four monomers in the asymmetric unit.

main-chain atoms in the wild-type protein is very small. The mean deviation from the main-chain atom positions ranges between 0.348 and 0.514 Å. When the side chains are included into the optimized-fit calculations, the r.m.s. deviation of atomic positions rises to 0.852 Å on average. A more complete description of the r.m.s. differences is presented in Table 3.

The metal coordination found in the Asn47Asp mutant is very similar, if not indentical to the one seen in the *Pseudomonas aeruginosa* wild-type zinc azurin (Nar *et al.*, 1992); a distorted tetrahedral array of four strongly bound ligands, the carbonyl O atom of Gly45, the N$^{\delta}$ of His46 and His117, and finally the S$^{\gamma}$ atom from Cys112 (see Table 4 and Fig. 7). Zinc binding to azurin, however, causes a structural adjustment of the polypeptide atoms in its immediate surroundings. More significant shifts are observed for residues 44 and 45. In particular, O45 moves *ca* 0.3 Å towards the Zn atom making the metal cage in the apical direction compressed. These differences between the Asn47Asp structure and the wild-type structure are shown in Fig. 8. The pronounced differences are statistically significant viewed against the measured precision in the Luzzati plot (Fig. 4).

The site-specific mutation was introduced at residue 47, which was determined to be a conserved asparagine residue (Rydén & Lundgren, 1976) in all the azurins and their analogues and, as a comparison, Asn38 is invariant in all the different plastocyanins. This residue is located directly in the proximity of the Cys112 ligand, at a distance of

about 5.5 Å from the metal site in the wild-type structure (Fig. 7). The side chain of Asn47 makes three hydrogen bonds, one with the main-chain group Thr113 NH($O^{\delta 1}$—NH), one with the side chain of Thr113($N^{\delta 2}$—$O^{\gamma 1}$) and a third hydrogen bond with one solvent water molecule, the latter two hydrogen bonds being bifurcated. The Asp47 side chain is tilted slightly with respect to Asn47 in the wild-type protein (Fig. 8), while both hydrogen bonds formed with the Thr113 moiety are preserved. A difference to the wild type is apparent in the solvent structure around the mutation site. While in the wild-type structure a third hydrogen bond to a water molecule is formed, we find, in addition, another ordered water molecule in the 8 Å-deep cavity (at the bottom of which lies Asp47). This

second water molecule forms one hydrogen bond to the first water molecule. A more extensive hydrogen-bond network is then formed as shown in Fig. 9. This difference might be because of the extra negative charge which makes a charge delocalization *via* hydrogen bonds necessary. Other differences such as the decreased distance of Asp47 $O^{\delta 1}$ to Cys112 S^{γ} (3.44 *versus* 3.52 Å) are within the limits of positional error and should, therefore, be considered insignificant.

Discussion

The metal coordination in zinc Asn47Asp azurin is identical to that previously determined for wild-type zinc azurin and is different compared to the copper site of wild-type azurin and other azurin mutants. The distance between the Zn atom and the carbonyl O atom of Gly45 is reduced to 2.36 Å (2.97 Å for Cu—O45) while the NNS coordination is retained. This results in a distorted tetrahedral coordination sphere around Zn^{II}. According to the rack-induced bonding concept as formulated by Gray & Malström (1983), the bound metal ion in metalloproteins is forced to adopt a coordination geometry determined by the rigid-peptide conformation. However, this structure and the previous zinc-azurin structure by Nar *et al.* (1992) show that, although the tight cluster of hydrogen bonds around the metal site in azurin prevents major conformational changes some smaller distortions of the backbone are seemingly allowed.

In general, the divalent zinc ion can be found in small-molecule structures with a variety of coordination numbers from coordination number 2 in $Zn(CH_3)_2$ to coordination number 8 in $(Ph_4As)_2$-$Zn(NO_3)_4$ (Drummond & Wood, 1970). Since there is no ligand-field stabilization effect in the Zn^{2+} ion because of the completed *d* shell, its stereochemistry is determined solely by consideration of size, electrostatic forces and covalent-bonding forces. In most cases the divalent Zn atom tends to assume the coordination number of 4.
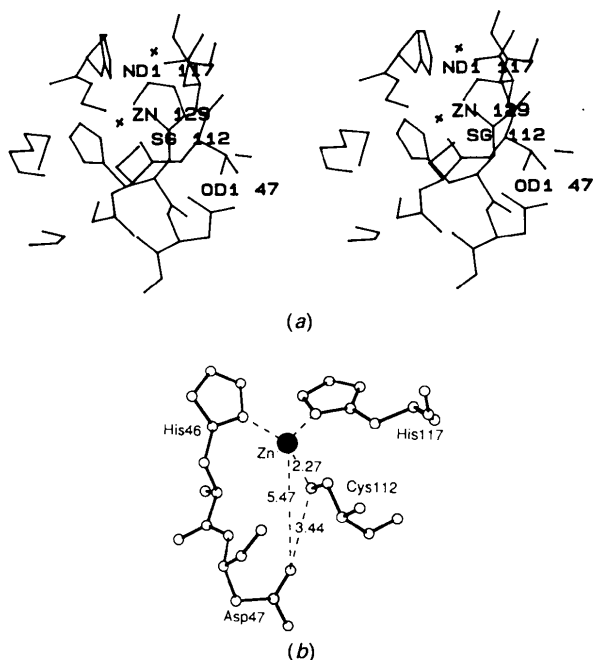

(a)

(b)

Fig. 7. (*a*), (*b*) Presentations of the mutation site Asp47 and the Zn atom and its binding pattern to the three major ligands His46, Cys112 and His117.
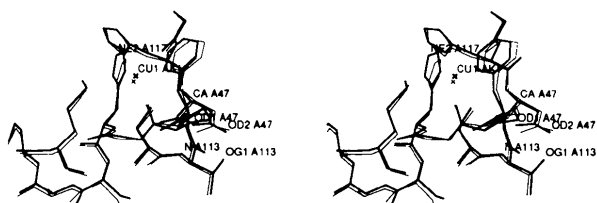

Fig. 8. A presentation of the differences in the metal site between wild-type azurin and mutated Asn47Asp zinc derivative. The superposition is based on a least-squares fit of the main-chain atoms.
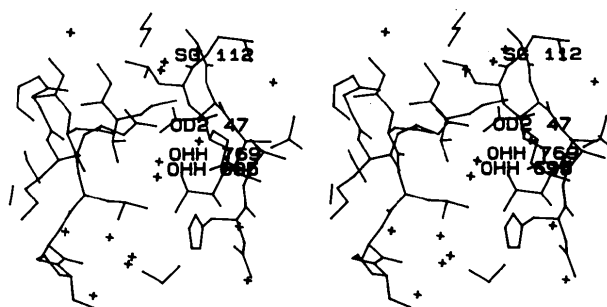

Fig. 9. A stereo plot of the 8 Å deep water-containing cavity in the proximity of the side chain of amino-acid residue Asp47.

Tetrahedral zinc coordination in proteins and enzymes by Cys, His and oxygen-donor ligands is relatively common (Vallee & Auld, 1990) but as was found from the zinc-containing azurin structure by Nar *et al.* (1992) the mixed NNSO coordination sphere in this structure is novel. In fact, this coordination sphere is seemingly rare for organometallic zinc structures in general. Consequently, in the Cambridge Structural Database (1992), there are only five crystallographic structures listed with a similar coordination motif (Liles, McPartlin & Tasker, 1977, 1987; Bourne & Taylor, 1980).

The mutation performed on the amino-acid residue Asn47 to become an aspartic acid was initiated because we were interested in finding out the impact of the hydrogen-bonding pattern and charge distribution in the vicinity of the metal site. Other mutations have previously been performed on the amino-acid residue Asn47 and, in the case of the mutation Leu47, it has not been possible to make copper bind in the metal site, a rather peculiar result for which we have no explanation as yet. The Asn47Leu mutant of *Alcaligenes denitrificans* azurin has, however, been isolated and characterized by Hoitink & Canters (1992). In their case, the Cu atom did bind to the protein and the protein consequently turned blue. The altered hydrogen-bonding pattern in this mutant did not affect the structure of the molecule nor its metal site. The most striking result was, however, the sharply increased reduction potential. These findings have led us to construct a double mutant (Asn47Leu, Met121Leu) showing the highest reduction potential so far measured on *Pseudomonas aeruginosa* azurin mutants (Pascher, Karlsson, Nordling, Malmström & Vänngård, 1993).

While in the Asn47Leu case the hydrogen-bond network was altered but charge effects were excluded, we have largely preserved the hydrogen-bonding scheme in the Asn47Asp azurin mutant while introducing a negative charge at roughly 5.5 Å from the metal site. The slight increase in reduction potential which we observe in Asn47Asp azurin is contradictory, however, to what should be expected in terms of a simple electrostatic model in which the effect of an additional negative charge close to the copper should stabilize the oxidized form of the protein and lower the midpoint potential. In order to determine statistically the most important physicochemical factors that are related to the variations of the reduction potential in different mutants, an investigation using the quantitative structure–property relationships method (Wold, 1979; Hellberg, Sjöström, Skagerberg & Wold, 1987) has been initiated and the results will be presented elsewhere.

Finally, it must be stated that the Asn47Asp mutation does not have any major effect on the zinc-site geometry, since the zinc coordination in our structure is very similar to the coordination in the wild-type azurin. Thus, compensatory effects of charge delocalization *via* hydrogen bonds might only play a role in tuning the redox potential in the present case.

In order to elucidate further the role of various amino acids in different positions in the peptide chain and their influence on the strain of the metal site and consequently the reduction potential we will continue the molecular biology program including cloning, expression and mutagenesis of the genes for blue copper proteins in connection with spectroscopic and diffraction measurements.

References

AASA, R. & VÄNNGÅRD, T. (1975). *J. Magn. Reson.* **19**, 308–315.

ADMAN, E. T. (1991). *Adv. Protein Chem.* **42**, 145–197.

ADMAN, E. T. & JENSEN, L. H. (1981). *Isr. J. Chem.* **21**, 8–12.

ADMAN, E. T., STENKAMP, R. E., SIEKER, L. C. & JENSEN, L. H. (1978). *J. Mol. Biol.* **123**, 35–47.

AINSCOUGH, E. W., BINGHAM, A.-G., BRODIE, A. M., ELLIS, W. R., GRAY, H. B., LEOHR, T. M., PLOWMAN, J. E., NORRIS, G. E. & BAKER, E. N. (1987). *Biochemistry*, **26**, 71–82.

AMBLER, R. P. & TOBARI, J. (1985). *Biochem. J.* **232**, 451–457.

BAKER, E. N. (1988). *J. Mol. Biol.* **203**, 1071–1095.

BEEUMEN, J. VAN, VAN BUN, S., CANTERS, G. W., LOMMEN, A. & CHOTHIA, C. (1991). *J. Biol. Chem.* **266**, 4869–4877.

BLAIR, D. F., CAMPBELL, G. W., SCHOONOVER, J. R., CHAN, S. I., GRAY, H. B., MALSTRÖM, B. G., PECHT, I., SWANSON, B. I., WOODRUFF, W. H., CHO, W. K., ENGLISH, A. M., FRY, H. A., LUM, V. & NORTON, K. A. (1985). *J. Am. Chem. Soc.* **107**, 5755–5766.

BOURNE, P. E. & TAYLOR, M. R. (1980). *Acta Cryst.* B36, 2143–2147.

BRÜNGER, A. T. (1990). *X-PLOR Manual.* Version 2.1. Yale Univ., New Haven, CT, USA.

Cambridge Structural Database (1992). Version 5.04. Univ. Chemical Laboratory, Lensfield Road, Cambridge, England.

CARTER, P. (1986). *Biochem. J.* **237**, 1–7.

CHOTHIA, C. & LESK, A. M. (1982). *J. Mol. Biol.* **160**, 309–323.

DRUMMOND, J. & WOOD, J. S. (1970). *J. Chem. Soc. A*, pp. 226–232.

EYRING, H., LUMRY, R. & SPIKES, J. D. (1956). *Mechanism of Enzyme Action*, edited by W. D. MCELROY & B. GLASS, pp. 123–136. Baltimore: John Hopkins Press.

FEE, J. A. (1975). *Struct. Bonding (Berlin)*, **23**, 1–60.

GRAY, H. B. & MALMSTRÖM, B. G. (1983). *Comments Inorg. Chem.* **2**, 203–209.

GROENEVELD, C. M. & CANTERS, G. W. (1985). *Eur. J. Biochem.* **153**, 559–564.

GUSS, J. M. & FREEMAN, H. C. (1983). *J. Mol. Biol.* **169**, 521–563.

HELLBERG, S., SJÖSTRÖM, M., SKAGERBERG, B. & WOLD, S. (1987). *J. Med. Chem.* **30**, 1126–1135.

HOITINK, C. W. G. & CANTERS, G. W. (1992). *J. Biol. Chem.* **26**, 13836–13842.

HOWARD, A. J., GILLILAND, G. L., FINZEL, B. C., POULOS, T. L., OHLENDORF, D. H. & SALEMME, F. R. (1987). *J. Appl. Cryst.* **20**, 383–387.

JONES, T. A. (1978). *J. Appl. Cryst.* **11**, 268–272.

JONES, T. A., ZOU, J.-Y., COWAN, S. W. & KJELDGAARD, M. (1991). *Acta Cryst.* A**47**, 110–119.

KARLSSON, B. G., NORDLING, M., PASCHER, T., TSAI, L.-C., SJÖLIN, L. & LUNDBERG, L. G. (1991). *Protein Eng.* **44**, 343–349.

KARLSSON, B. G., PASCHER, T., NORDLING, M., ARVIDSSON, R. H. A. & LUNDBERG, L. G. (1989). *FEBS Lett.* **246**, 211–217.

KARLSSON, B. G., TSAI, L.-C., NAR, H., LANGER, V. & SJÖLIN, L. (1993). In preparation.

LILES, D. C., MCPARTLIN, M. & TASKER, P. A. (1977). *J. Am. Chem. Soc.* **99**, 7704–7705.

LILES, D. C., MCPARTLIN, M. & TASKER, P. A. (1987). *J. Chem. Soc. Dalton Trans.* pp. 1631–1636.

LINDSKOG, S. & MALMSTRÖM, B. G. (1962). *J. Biol. Chem.* **237**, 1129–1137.

LUMRY, R. & EYRING, H. (1954). *J. Phys. Chem.* **58**, 110–120.

LUZZATI, V. (1952). *Acta Cryst.* **5**, 802–810.

MALKIN, M. & MALMSTRÖM, B. G. (1970). *Adv. Enzymol.* **33**, 177–243.

MALMSTRÖM, B. G. (1965). *Oxidases and Related Redox Systems*, Vol. 1, edited by T. E. KING, H. S. MASON & M. MORRISON, pp. 207–216. New York: Wiley.

MALMSTRÖM, B. G. & VÄNNGÅRD, T. (1960). *J. Mol. Biol.* **2**, 118–124.

MATTHEWS, B. W. (1968). *J. Mol. Biol.* **33**, 491–497.

NAR, H., HUBER, R., MESSERSCHMIDT, A., FILIPPOU, A. C., BARTH, M., JAQUINOD, M., VAN DE KAMP, M. & CANTERS, G. W. (1992). *Eur. J. Biochem.* **205**, 1123–1129.

NAR, H., MESSERSCHMIDT, A., HUBER, R., VAN DE KAMP, M. & CANTERS, G. W. (1991*a*). *J. Mol. Biol.* **218**, 427–447.

NAR, H., MESSERSCHMIDT, A., HUBER, R., VAN DE KAMP, M. & CANTERS, G. W. (1991*b*). *J. Mol. Biol.* **221**, 765–776.

NORRIS, G. E., ANDERSON, B. E. & BAKER, E. N. (1986). *J. Am. Chem. Soc.* **108**, 2784–2785.

PASCHER, T. (1992). PhD thesis, Univ. of Göteborg, Sweden.

PASCHER, T., BERGSTRÖM. J., MALMSTRÖM, B. G., VÄNNGÅRD, T. & LUNDBERG, L. G. (1989). *FEBS Lett.* **258**, 266–268.

PASCHER, T., KARLSSON, B. G., NORDLING, M., MALMSTRÖM, B. G. & VÄNNGÅRD, T. (1993). *Eur. J. Biochem.* In the press.

PETRATOS, K., DAUTER, Z. & WILSON, K. S. (1988). *Acta Cryst.* B**44**, 628–636.

RAMAKRISHNAN, C. & RAMACHANDRAN, G. N. (1965). *Biophys. J.* **5**, 909–933.

RYDÉN, L. (1984). *Copper Proteins, Copper Enzymes*, edited by R. LONTIE, pp. 157–182. Boca Raton, Florida: CRC Press.

RYDÉN, L. & LUNDGREN, J. O. (1976). *Nature (London)*, **261**, 344–346.

SAILASUTA, N., ANSON, F. C. & GRAY, H. B. (1979). *J. Am. Chem. Soc.* **101**, 455–458.

SOLOMON, E. I. & LOWERY, M. D. (1993). *Science*, **259**, 1575–1581.

STANDZENIEKS, P., RINDBY, A. & SELIN, E. (1978). *Nucl. Instrum. Methods*, **153**, 269–276.

STANDZENIEKS, P. & SELIN, E. (1979). *Nucl. Instrum. Methods*, **165**, 63–65.

STEIGEMANN, W. (1974). PhD thesis, Technische Univ. München, Germany.

VALLEE, B. L. & AULD, D. S. (1990). *Biochemistry*, **29**, 5647–5659.

VALLEE, B. L. & WILLIAMS, R. J. P. (1968). *Proc. Natl Acad. Sci USA*, **59**, 498–505.

WILSON, A. J. C. (1949). *Acta Cryst* **2**, 318–321.

WIRENGA, R. K., KALK, K. H. & HOL, W. G. J. (1987). *J. Mol. Biol.* **198**, 109–121.

WOLD, S. (1979). *Technometrics*, **20**, 379–405.